Research article

Philipp Grimm, Gary Razinskas, Jer-Shing Huang* and Bert Hecht*

Driving plasmonic nanoantennas at perfect impedance matching using generalized coherent perfect absorption

https://doi.org/10.1515/nanoph-2021-0048
Received February 3, 2021; accepted April 1, 2021;
published online April 26, 2021

Abstract: Coherent perfect absorption (CPA) describes the absence of all outgoing modes from a lossy resonator, driven by lossless incoming modes. Here, we show that for nanoresonators that also exhibit radiative losses, e.g., plasmonic nanoantennas, a generalized version of CPA (gCPA) can be applied. In gCPA outgoing modes are suppressed only for a subset of (guided plasmonic) modes while other (radiative) modes are treated as additional loss channels - a situation typically referred to as perfect impedance matching. Here we make use of gCPA to show how to achieve perfect impedance matching between a single nanowire plasmonic waveguide and a plasmonic nanoantenna. Antennas with both radiant and subradiant characteristics are considered. We further demonstrate potential applications in background-free sensing.

Keywords: coherent perfect absorption; impedance matching; plasmonics; nanoantenna.

***Corresponding authors: Bert Hecht**, Nano-Optics & Biophotonics Group, Department of Experimental Physics 5, University of Würzburg, Am Hubland, 97074 Würzburg, Germany; and **Jer-Shing Huang**, Leibniz Institute of Photonic Technology, Albert-Einstein-Str. 9, 07754 Jena, Germany; Institute of Physical Chemistry and Abbe Center of Photonics, Friedrich-Schiller-Universität Jena, 07743 Jena, Germany; Research Center for Applied Sciences, Academia Sinica, 128 Sec. 2, Academia Road, Nankang District, 11529 Taipei, Taiwan; and Department of Electrophysics, National Chiao Tung University, 30010 Hsinchu, Taiwan, E-mail: hecht@physik.uni-wuerzburg.de (B. Hecht), jer-shing.huang@leibniz-ipht.de (J.-S. Huang), https://orcid.org/0000-0002-4883-8676 (B. Hecht), https://orcid.org/0000-0002-7027-3042 (J.-S. Huang)
Philipp Grimm and Gary Razinskas, Nano-Optics & Biophotonics Group, Department of Experimental Physics 5, University of Würzburg, Am Hubland, 97074 Würzburg, Germany, E-mail: pgrimm@physik.uni-wuerzburg.de (P. Grimm), razinskas_g@ukw.de (G. Razinskas). https://orcid.org/0000-0003-4744-7005 (P. Grimm)

1 Introduction

Perfect absorption of selected frequencies of coherent light is a special condition that can occur in systems that scatter light and possess lossy resonances. Such coherent perfect absorption (CPA) is based on complete destructive interference of all outgoing modes and corresponds to the time-reversed process of lasing at threshold [1–6]. At the CPA condition incoming modes are completely absorbed by the system and completely converted to other forms of energy, usually heat. Naturally, CPA occurs at Fabry–Perot resonances of the lossy resonator. This is because the multiple reflections which accompany such resonances can lead to perfect destructive interference between the first reflected wave and all subsequent outgoing waves. This requires matching both their total phase and amplitude. Technically, a CPA condition corresponds to a zero eigenvalue of the scattering matrix associated with phase singularities located on the emitted mode's dispersion characteristic in the complex wave vector plane.

Being lossy is a rather natural property of plasmonic systems, which are therefore perfectly suited to exhibit CPA. Indeed, CPA has previously been proposed or observed in systems combining localized plasmonic resonators with photonic modes in dielectrics or free space [7–15]. Compared to dielectric Fabry–Perot-type resonators originally used for CPA, plasmonic resonators, i.e., optical antennas, exhibit much more flexibility because they offer a variety of resonances whose properties can be tailored to exhibit e.g. radiant or subradiant characteristics. In any case, radiative losses cannot be ignored and even for subradiant modes contribute significantly to the overall losses of such an antenna with respect to the driving guided modes. Yet, in the original concept of CPA radiation losses are usually neglected.

Here we show that the concept of CPA, which requires at least one eigenvalue of the complete scattering matrix to vanish, can be generalized to situations where this applies only to a sub matrix. As an example, we consider a semi-infinite single-mode gold plasmonic nanowire which is

coupled to a single gold nanorod antenna via a gap. At least one zero eigenvalue of the scattering matrix is required only for the guided wire modes, while the infinite number of radiative modes of the nanorod is treated as losses. By doing so, we sacrifice the instructive, but practically not very relevant correspondence of CPA to the time-reversed version of lasing at threshold. On the other hand, generalized CPA (gCPA) can now be applied to any resonant absorber with both radiative and nonradiative loss channels, possibly including the absorption of light by quantum emitters. In the case of a single nanorod studied here, obviously, the condition of gCPA corresponds to perfect impedance matching between the nanorod antenna and the nanowire transmission line since the incoming plasmonic mode is perfectly absorbed without any reflection [16–19]. Achieving perfect impedance matching is intrinsically challenging in plasmonic nanostructures because of the mismatch between the wavelength of guided plasmons and free space waves [20]. Depending on the chosen nanorod resonance we achieve under perfect impedance matching either strong far-field radiation or generation of heat.

In the proposed gCPA, the choice of the subspace in the output vector is flexible, depending on the application of interest. The subspace treatment is based on the fact that a global scattering matrix (S-matrix) may use a basis of guided modes and radiative modes. In the traditional formulation of CPA, only waveguide modes were considered and thus the S-matrix contained the coupling between guided input and output modes only. For the settings explored in the work of Stone [1], this ignoring of possible radiative modes is fully justified, whereas in the case of nanoplasmonics it is not. In this sense, our approach is a generalization of CPA. When the guided plasmon has zero reflection at the end of the wire we call it gCPA because the analysis of this effect follows the logic of Stone's CPA. Yet, the energy fed to the nanorod is not completely dissipated to heat, but some radiation occurs such that guided modes only are insufficient to capture the complete behavior of the system. While the example discussed here is specific, the underlying concept is more general than the original CPA. Recently, Sweeny and Stone reported a generalized theory of reflectionless scattering modes (RSM) [5, 6], which allows for reaching zero reflection of the selected input modes by evaluating the eigenvalue of the corresponding subset of the scattering matrix. The reradiation from the system can be considered as one of the complementary output channels. While the RSM theory may also be applied to address resonators with radiative loss, the gCPA presented in this work was developed independently to address the coupling of a guided subwavelength surface plasmon mode to an optical nanoantenna. The underlying physics responsible for the zero reflection in this deep subwavelength system is clearly explained. We demonstrate the possibility of background-free sensing using a disturbed gCPA condition and coherent control of the radiation from a nanorod. Our findings establish gCPA as a tool in plasmonic nanocircuitry and nanoantenna design and technology.

2 Concept of generalized coherent perfect absorption

With dielectric waveguides and resonators, such as photonic waveguides feeding into a lossy cavity, the only dissipation mechanism in CPA is heat generation inside the cavity. Far-field radiation is not considered. Hence, a scattering matrix consisting of the coupling coefficients between the incoming and outgoing guided modes fully captures the modal conversion and energy exchange within and between the resonator and waveguides. However, the situation is different when it comes to plasmonic nanoantennas, where the oscillating surface plasmon leads to radiative decay in addition to the nonradiative loss into heat. In this case, the concept of gCPA would allow us to concentrate on the perfect absorption of the input mode of interest without fulfilling the requirements of CPA for the complete system. As an example, we illustrate the concept of gCPA with the case of a plasmonic nanoantenna driven by two semi-infinite single-mode plasmonic nanowires (Figure 1). The resonator exhibits both Ohmic damping and far-field radiation. The latter can be expressed as a superposition of suitable free-space modes, e.g., plane waves propagating in different directions.

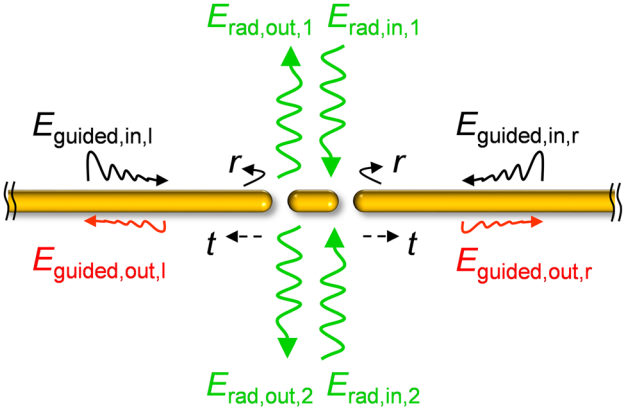

Figure 1: Sketch of a symmetric wire–rod–wire system. In general, guided surface plasmons E_{guided} as well as radiative modes E_{rad} have to be used as incoming and outgoing modes. Within the generalized CPA formalism in this work, only the subset of guided surface plasmons is considered as incoming modes.

The total scattering matrix of the wire-rod-wire system in Figure 1 is defined by

$$\begin{pmatrix} E_{\text{guided, out, }l} \\ E_{\text{guided, out, }r} \\ E_{\text{rad, out, 1}} \\ E_{\text{rad, out, 2}} \\ \vdots \end{pmatrix} = S_{\text{global}} \begin{pmatrix} E_{\text{guided, in, }l} \\ E_{\text{guided, in, }r} \\ E_{\text{rad, in, 1}} \\ E_{\text{rad, in, 2}} \\ \vdots \end{pmatrix} \tag{1}$$

connecting *all* incoming with *all* outgoing modes. The four coefficients describing the coupling between the guided modes occupy the upper left corner of the scattering matrix as a two-by-two matrix,

$$S_{\text{global}} = \begin{pmatrix} \begin{bmatrix} r & t \\ t & r \end{bmatrix} & \begin{matrix} c_{l1} & c_{l2} \\ c_{r1} & c_{r2} \end{matrix} & \cdots \\ \begin{matrix} c_{1l} & c_{1r} \\ c_{2l} & c_{2r} \\ \vdots & \vdots \end{matrix} & \begin{matrix} d_{11} & d_{12} \\ d_{21} & d_{22} \\ \vdots & \vdots \end{matrix} & \begin{matrix} \cdots \\ \cdots \\ \ddots \end{matrix} \end{pmatrix} \tag{2}$$

Here, r and t are the reflection and transmission coefficients of guided surface plasmons at the nanorod, the c_{ij} are coefficients describing the modal coupling between surface plasmons and radiative modes, and d_{ij} establish the coupling among radiative modes. In this generalized framework, the "complete" CPA requires to find a condition for which an eigenvalue of the *entire* scattering matrix becomes zero. This means *all* outgoing channels, guided modes and radiation, are turned to zero simultaneously. Achieving such complete CPA can be experimentally challenging or even impossible for resonators with radiative loss, such as nanoantennas.

In this work, the input and output modes we are interested in are the left-propagating and right-propagating fundamental guided modes on a plasmonic nanowire. All other modes are treated as loss channels, including the radiation of the nanoantenna. The input field vector that is multiplied with the scattering matrix therefore only contains finite values for the top two components in Eq. (1). All the other components are set to zero. Now, gCPA requires only finding and zeroing the eigenvalue of the subset of the resulting upper left two-by-two matrix, as marked by the square brackets in Eq. (2), which describes the coupling between the guided modes only. Since the major part of the scattering matrix which connects the radiative modes is not considered in the required diagonalization the coupling to radiative modes will in general not be zero, meaning that complete CPA of the whole system is in general not achieved. The coupling to radiative modes is treated as a part of the loss of the guided plasmonic modes. As we will show in the following, by choosing the nanoantenna to be subradiant or superradiant, the amount of radiation losses can be controlled to a large degree. Generalized CPA, i.e., a zero eigenvalue of a submatrix, occurs if the energy from a few incoming guided wire plasmons is entirely converted to other forms of energy, no matter radiative or nonradiative, featuring the zero reflection of the input modes. This provides a practical route to find the condition for perfect impedance matching between plasmonic waveguides and plasmonic nanoantennas in nanocircuitry.

3 Perfectly impedance-matched nano antenna using generalized coherent perfect absorption

In the following, we demonstrate that the concept of gCPA allows us to find the condition for perfect impedance matching between a single wire plasmonic waveguide and nanorod optical antenna. At this condition, the guided wire plasmons are completely injected into the antenna without any reflection and the injected power is branched into radiative and nonradiative loss, depending on the antenna mode and excitation conditions.

The system under study consists of a semi-infinite gold nanowire with a circular cross section (30 nm diameter) in the vacuum in the near infrared regime (310–400 THz, corresponding to vacuum wavelength 749–967 nm). The wire is terminated by a hemispherical end cap. A gold nanorod with the same diameter and end caps is coupled to the nanowire over a few nanometer wide gap (see Figure 2a). Throughout this work, the minimum gap width studied is 3 nm. Since all gaps are sufficiently large we neglect quantum effects. For subnanometer gaps, more sophisticated methods might be needed to obtain the fundamental reflection and transmission coefficients under the influence of quantum effects. As long as these coefficients could be obtained, the formalism would work in the same way. Owing to the relatively small wire diameter compared to the vacuum wavelength, the nanowire supports only the fundamental plasmonic TM_0 eigenmode [21, 22]. Its transverse mode profile is displayed in the inset of Figure 2a. The complex propagation constant

$$k = \beta + i\alpha \tag{3}$$

is found using the finite-difference frequency-domain method (MODE Solutions, Lumerical Solutions Inc.) [23]. Here, i is the imaginary unit, $\beta = 2\pi/\lambda_{\text{eff}}$ is the propagation constant with λ_{eff} the effective wavelength, and α is the field decay constant because of Ohmic losses. The dielectric function of gold is modeled using single-crystal data [24]. The obtained eigenmode is used as a source in three-dimensional finite-difference time-domain simulations

(FDTD Solutions, Lumerical Solutions Inc.). Taking plasmon reflection at the wire termination into account the electric near-field intensity distribution along the semi-infinite wire is [25, 26]

$$|E(x)|^2 = \left|E_0\left[e^{ikx} + e^{ik(x_0-x)}\Gamma e^{ikx_0}\right]\right|^2, \quad (4)$$

where E_0 is the initial amplitude of the mode, x is the spatial coordinate in the propagation direction, x_0 is the distance between the mode source injection point at $x = 0$ and the end of the cylindrical part of the wire at $x = 2985$ nm, and Γ is the complex reflection coefficient obtained by fitting the simulated standing wave pattern of the electric near-field intensity 5 nm away from the wire surface with Eq. (4). This yields Γ as the only free parameter. Since the mode reflection is very sensitive to the exact condition of the wire termination [27, 28], the nanorod coupled via the nanosized gap can alter the reflection coefficient and the standing wave pattern drastically. Figure 2b shows two distinctively different exemplary near-field standing wave patterns corresponding to the absence of a nanorod and a specifically chosen rod length to be discussed below. In absence of a vicinal nanorod a pronounced standing wave pattern is observed corresponding to a high reflectivity ($|\Gamma| = 95\%$). For a nanorod length of 346 nm, nearly zero reflectivity is observed, accompanied by strong energy localization on the nanorod. The absence of the reflection corresponds to perfect impedance matching between the nanowire (transmission line) and the nanorod (load) and suggests an effective scheme to drive the nanorod antenna via a single-wire transmission line (see Visualization 1 and Section I of Supplementary Material). In optical nanocircuitry, the characteristic impedance is determined by the electromagnetic fields of the guided mode on the nanowire. The degree of impedance matching, described by the complex reflectivity Γ, can be evaluated by characterizing the standing waves of the optical near field around the nanowire waveguide termination. Once the characteristic impedance of the guided mode and the reflectivity at a given termination are known, the impedance of the load, i.e., the nanoantenna, can be calculated using the complex reflectivity Γ [25].

In the following, we show that the observed zero reflectivity corresponds to a gCPA condition of the guided plasmonic mode that can be achieved for both a

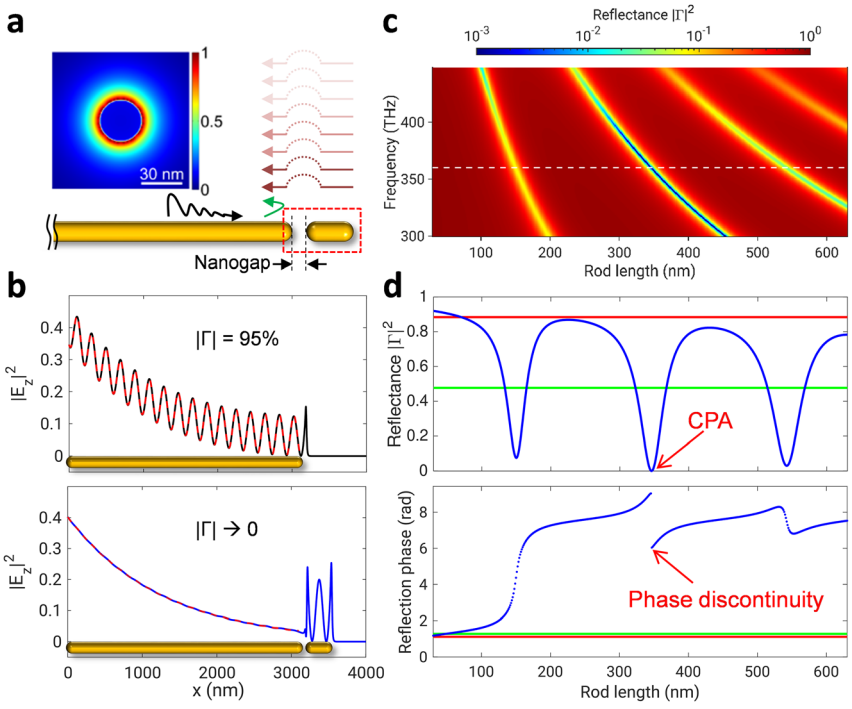

Figure 2: (a) Reflection of the right propagating guided plasmonic mode (black arrow) at the termination of a gold nanowire. The total mode reflection at the wire termination (red dashed rectangle) is determined by the interference between the directly reflected mode at the gap (green arrow) and a series of coherent transmissions from the mode oscillating on the nanorod (dark red arrows). See Section II of Supplementary Material for details. Inset: modal profile of the guided wire mode. (b) Simulated standing wave patterns of the guided wire mode (electric near-field intensity) for a termination open to vacuum (upper panel) and facing a 346-nm nanorod (lower panel) via a 5-nm gap. The red dashed lines show the fits of Eq. (4) to these standing wave patterns (FDTD) using the complex reflectivity Γ as the only free fit parameter. (c) Calculated reflectance ($|\Gamma|^2$) as a function of the nanorod length and frequency. The gap is 4 nm. (d) Reflection intensity (upper panel) and phase (lower panel) as a function of the nanorod length at 360 THz, marked by the white dashed line in (c). The red and green horizontal lines mark the reflectance and phase of a termination open to vacuum and a gap in an infinitely long wire, respectively.

superradiant and a subradiant resonance of the nanorod. This offers the opportunity to control the branching ratio of the absorbed power to either far-field radiation or absorption. We describe the overall reflectivity of the nanowire termination using a semi-analytical approach, in which the gap-coupled nanorod is considered as an effective Fabry–Perot resonator [29, 30]. The reflectivity of the nanorod termination can then be calculated by summing up an infinite geometrical series involving the open-end reflectivity and the reflection and transmission at a gap between two semi-infinite wires (see Section II of Supplementary Material). These three parameters are determined numerically by means of FDTD simulations for a range of frequencies and gap widths as described in Supplementary Material. The resulting analytical expression allows us to instantaneously calculate the overall reflectivity of the wire–rod system. For further analysis, we note that the overall reflectivity also corresponds to the scattering 'matrix' of the system for the subset of guided modes which is a scalar for the 1D single-mode case considered here. Perfect destructive interference, i.e., zero reflectivity, requires the directly reflected mode (green arrow, Figure 2a) and the transmitted mode, consisting of the infinite sum of transmitted waves over the gap (dark red arrows, Figure 2a), to have opposite phases and equal amplitudes. To achieve this, the nanorod must provide just the right amount of loss and the gap must be chosen correctly to transmit a just sufficient portion of the mode for each round trip. In this regard, the length-dependent Ohmic losses of the plasmonic waveguide indeed become important and beneficial to enable unidirectional nanoscale gCPA.

Figure 2c shows the calculated reflectance (squared reflection amplitude, $|\Gamma|^2$) as a function of nanorod length at various frequencies for a fixed gap of 4 nm. Multiple local minima are obtained at different orders of nanorod resonances. Indeed, the second-order minimum reaches zero reflection, i.e., gCPA as we prove below. Interestingly, all the rod lengths for which reflection minima occur coincide with those of solitary nanorods showing a scattering resonance at that wavelength as if the proximity of the nanowire did not perturb the resonance of the nanorod. This coincidence marks a special "nonbonding" condition, where the phase of the electric field on opposing sides of the gap exhibits $\pi/2$ difference (see Section III of Supplementary Material). gCPA must show up at the "nonbonding" resonant rod length because CPA means no reflection and thus no charge accumulation at the semi-infinite wire end as if the wire was continuous. The nonbonding condition with appropriate loss offers the necessary phase and amplitude for perfectly destructive interference of the reflected mode. Another interesting feature is that gCPA is not associated with specific resonance orders. For example, at 440 THz, the smallest reflection occurs at the first-order resonance of the nanorod. At 360 THz (see Figure 2d), the nanorod's second-order resonance leads to the lowest reflection intensity. This suggests the flexibility to achieve gCPA with even and odd resonance orders and thus the possibility to select the loss mechanisms, as will be discussed later.

To distinguish good absorption (local reflection minima) from perfect absorption (gCPA), we investigate the continuity of the reflection phase. Figure 2d displays the reflectance and the reflection phase at 360 THz as a function of the nanorod length. The first, partial reflection dip, observed at nanorod length = 153 nm, exhibits a narrow pseudo Lorentzian line shape. The corresponding phase transition is steep but still continuous. The second reflection minimum at a rod length of 346 nm (see Figure 2b, lower panel) approaches zero, i.e., truly perfect absorption. The corresponding phase changes discontinuously. We would like to emphasize that this phase jump does not originate from an irrelevant 2π jump. It is caused by the vortex-like phase singularity (Figure 3a) which accompanies the zero reflectance of the gCPA state. A meaningless 2π jump would not give rise to such a singularity. The difference between a local minimum and a truly zero reflection because of CPA is that true CPA happens when the phase singularity hits the dispersion curve of the guided mode. If the phase singularity is close but does not exactly reside on the dispersion curve of the guided mode, the reflectance would just be a local minimum with a smooth transition of phase. In numerical simulations, a finite reflectance is inevitable due to limited finite mesh size and frequency step used in the simulations. In reality, the resolution is limited by the diameter of an atom (the smallest spatial step) and the frequency bandwidth of the source. The narrow bandwidth of the gCPA dip implies that ultrashort pulsed excitation with broad bandwidth is not compatible with gCPA.

4 Shifting the phase singularity on the complex wave vector plane

To prove that we indeed observe a generalized version of CPA, in Figure 3 we plot the reflectance and reflection phase over the complex wavevector plane [1, 31] since the attenuation constant α of the guided plasmonic TM_0 eigenmode may in principle be tuned by adding gain or additional absorption losses. For the selected range of

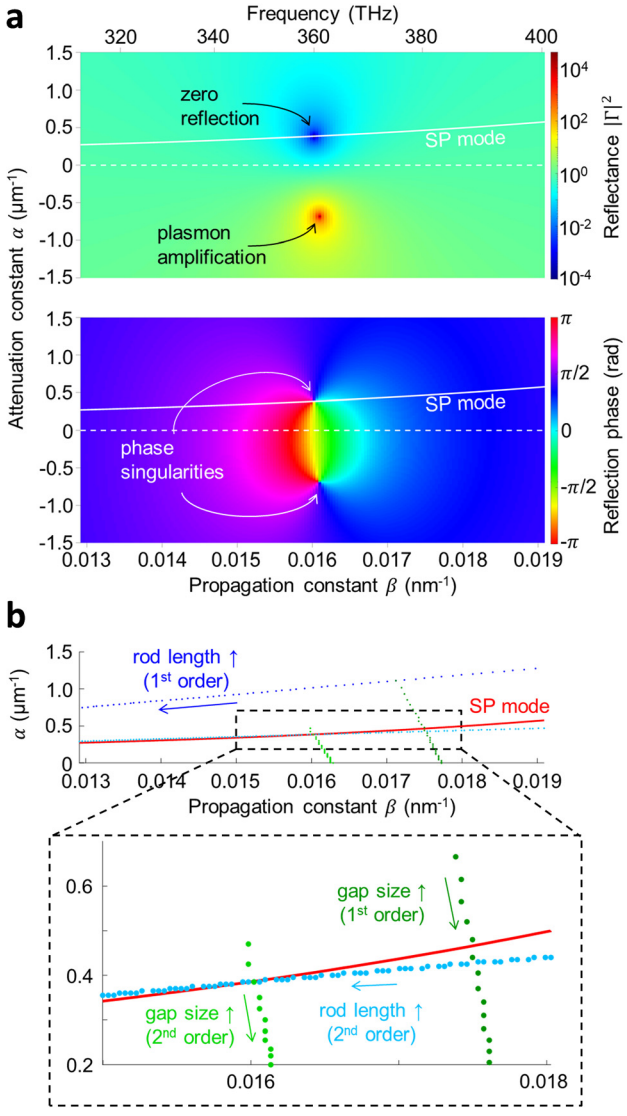

Figure 3: (a) The reflectance (upper panel) and reflection phase (lower panel) plotted over the complex wavevector plane for a specific terminal condition (rod length = 346 nm, gap = 4 nm), at which one of the phase singularities hits the dispersion curve of the guided mode, leading to zero reflection for one specific value of β. β and α are the real and imaginary parts of the wavevector. Negative α represents gain. (b) Upper panel: trajectories of the reflection phase singularities of the first-order and second-order nanorods resonance upon sweeping the gap size (increment 0.5 nm per dot) and nanorod length (increment 1 nm). Dark blue and dark green dots mark the trajectories of the phase singularity of the first-order resonance upon increasing the rod length (126–187 nm) and gap size (4–19 nm), respectively. Light blue and light green dots mark the trajectories of the phase singularity of the second-order resonance upon sweeping the rod length (290–431 nm) and gap size (3–20 nm), respectively. The red solid curve depicts the allowed α and β for the TM_0 mode on the nanowire. Lower panel: enlarged plot corresponding to the area marked by the dashed rectangle in the upper panel.

frequencies, the reflectivity displays a zero and a pole of its amplitude accompanied by phase singularities in the positive and negative α range, respectively. Further poles and zeros exist for each order of Fabry–Perot resonances of the nanorod (not shown). The plasmonic mode dispersion relation can be used to derive a relation between the propagation constant β and the damping α of the guided TM_0 mode (see Section IV of Supplementary Material). This relation is also plotted as a white solid line (SP mode) into the same complex wavevector plane. To achieve zero reflection, the phase singularity corresponding to zero reflectivity must reside on this curve describing allowed α and β combinations of the mode [32], such as the case displayed in Figure 3a. By changing the geometry of the termination, such as the gap size and nanorod length, the position of the phase singularities can be moved freely within the complex wavevector plane.

Figure 3b shows the trajectories of the phase singularities of the first-order and second-order resonances of the nanorod upon increasing the gap size and the rod length. While increasing the nanorod length shifts the phase singularities towards lower propagation constant, increasing the gap size mainly moves the singularity towards smaller attenuation constants. Within the experimentally accessible range of geometrical parameters, multiple singularities corresponding to different Fabry–Perot resonance orders of the nanorod are available. This allows us to rationally design a wire-rod system to achieve gCPA using super radiant or subradiant nanorod resonances, offering the opportunity to choose the dissipation mechanism for the absorbed energy. Thus, the gCPA analysis on the complex wavevector plane serves as a theoretical design tool for perfect impedance matching. The transfer matrix calculations yield fast results and avoid time-consuming numerical parameter sweeps. The good agreement between semi-analytical and purely numeric results for reflection amplitude and phase is demonstrated in Figure S2 of the Supplementary Material. A movie showing the motion of the phase singularities and the crossing of the mode dispersion, accompanied by the reflectance spectrum, is provided in Visualization 2 (see Section V of Supplementary Material for video description). Another important feature seen in Figure 3 is the phase singularity point in the lower half of the complex plane, where the attenuation constant α is negative. This phase singularity is associated with a reflectivity pole. For negative α the guided mode is amplified, suggesting the possibility of surface plasmon amplification by stimulated emission [9, 33, 34].

5 Exemplary applications of generalized coherent perfect absorption

The gCPA approach developed in this work offers a broad range of applications. In principle, it can be applied to study the coupling of any guided mode into lossy cavities where the total loss may include radiative channels. In particular, structures consisting of discrete elements are straightforward to treat as they are composed of elementary reflection and transmission events. In the following, we will discuss two applications of gCPA in plasmonic nanocircuitry, (i) driving bright or dark nanoantenna modes with perfectly matched impedance and (ii) background-free nanoscale sensing. Figure 4a shows the efficiency of radiative and nonradiative loss of a unidirectional gCPA-driven single nanorod in the first and second-order resonance. The same quantities of the open end of a semi-infinite nanowire are also plotted for reference. According to the symmetry of the currents on the nanorod, the first-order and second-order resonances are super-radiant and subradiant, respectively. Therefore, gCPA based on the first-order resonance (rod length = 157 nm and gap = 9 nm) results in 50% far-field radiation efficiency, whereas CPA achieved with the second-order resonance (rod length = 346 nm, gap = 5 nm) leads to 85% nonradiative energy dissipation into heat. Obviously, these values could be further improved by optimized antenna designs.

Two-port CPA using photonic modes with dielectric or plasmonic resonators has been used to demonstrate coherent control of light with light without using nonlinear effects [2, 7, 13, 14]. Guided plasmons on two plasmonic nanowires sandwiching one nanorod resonator can also be used to realize two-port gCPA [35] (see Section VI of Supplementary Material). With gCPA based on a super-radiant resonance mode, the relative phase of the two plasmon inputs can be used to coherently control the radiation of the plasmonic nanorod, i.e., to control the emission of a plasmon-driven transmitting optical nanoantenna by surface plasmon without using a nonlinear process.

For sensing applications, we use the subradiant nanorod resonance (rod length 346 nm, gap 5 nm) to achieve gCPA. Tiny perturbations of the nanorod's terminal conditions will shift the phase singularity in the complex plane and lead to the destruction of gCPA. As a result, a finite reflection against a completely dark background can be detected with high signal-to-background contrast, similar to the case of dark-field scattering or single-molecule fluorescence detection. Assuming that the major source of noise in an experiment is shot noise, which is proportional to the square root of the signal intensity, the signal-to-noise (S/N) ratio is proportional to the amplitude of the reflection. It should be noted, though, that the amplitude cannot be increased arbitrarily by increasing the input intensity due to local heating of the nanorod. In Figure 4b, we compare the change of the reflection amplitude upon local perturbations of a wire-rod system with that of a bare single wire probe. A perturbation is introduced by approaching a tiny dielectric glass nanosphere (diameter = 20 nm) to the termination

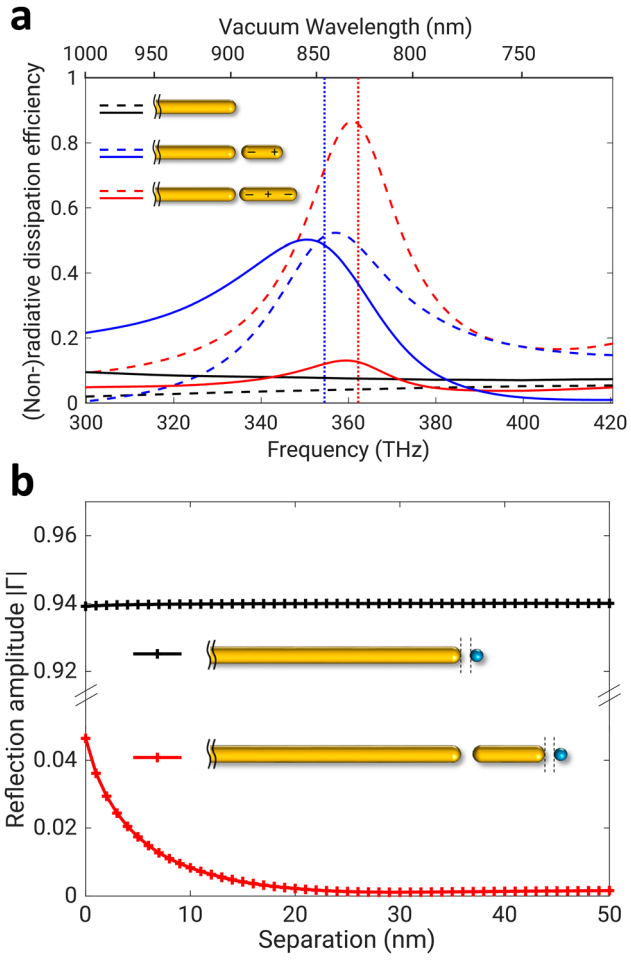

Figure 4: (a) Radiative (solid lines) and non-radiative (dashed lines) dissipation efficiency of gCPA-driven nanorod at the first-order (blue) and second-order resonances (red). The radiative and non-radiative dissipation efficiencies of the open end of a semi-infinite wire are also plotted for reference (black). The vertical dotted lines indicate the gCPA frequencies for first and second order resonances. Legends also include the charge distribution on the nanorods for first-order and second-order resonances. (b) Comparison of the reflection amplitude to a local perturbation (approaching dielectric sphere, diameter 20 nm) of a simple wire sensor (black) compared to a gCPA wire–rod sensor (red). For the latter, a pronounced change in reflection amplitude is observed for separations below 10–20 nm.

(inset of Figure 4b). The wire-rod system used here shows gCPA based on the subradiant second-order resonance, i.e., the second dip in Figure 2d. There is a rapid increase of the reflection amplitude as the silica nanosphere approaches the nanorod along the wire axis to a distance less than 20 nm. A pronounced nonlinear increase in the reflection amplitude is obtained when the separation is below 10 nm, showing ultimate sensitivity to perturbations in close vicinity of the probe. The analytically predicted reflectivity increase of the wire–rod system is perfectly reproduced by FDTD simulations (data not shown). We conceive that even attachment or detachment of single proteins should be detectable as a notable increase in reflectivity [36–38].

6 Conclusion

In conclusion, at the example of a semi-infinite plasmonic nanowire terminated by a gold nanorod, we present a new type of nanoscale, near-field energy transfer and perfect absorption based on a generalized CPA concept. We demonstrate that tuning the geometry of the nanorod can be used to deterministically move the reflectivity phase singularity in the complex wavevector plane. This allows us to find zero eigenvalue conditions for the selected subset of guided plasmonic modes of the scattering matrix. Since for gCPA no reflection occurs, the condition also corresponds to perfect impedance matching of the guided surface plasmon with respect to the nanorod antenna. The gCPA condition completely cloaks the wire termination and virtually decouples the nanorod from the feeding structure, i.e., a nonbonding condition. Thus gCPA allows injecting power to an optical nanoantenna to compensate the loss so that the antenna resonates continuously without damping, offering infinite quality factor at the resonant frequency. We further demonstrated that the gCPA condition is very sensitive to changes in the local environment and thus useful for background-free ultrasensing. A correctly designed nanowire-rod system could also serve as a probe for near-field sensing. Furthermore, we demonstrate the coherent control of nanoantenna radiation using two-port gCPA. Using the concept of gCPA is necessary for systems in which radiative losses may occur, e.g., plasmonic nanoresonators and quantum emitters. The generalization causes a breakdown of the equivalence between time-reversed lasing at threshold and CPA, although a SPASER condition (reflectivity pole) is still predicted if the loss on the nanorod is turned into gain.

Acknowledgments: We thank Tobias Helbig and Tobias Hofmann for pointing to the transfer matrix formalism, as well as Thorsten Feichtner and René Kullock for fruitful discussions. We also acknowledge the Würzburg-Dresden Cluster of Excellence on Complexity and Topology in Quantum Matter - ct.qmat (ST 046 2019).

Author contributions: All the authors have accepted responsibility for the entire content of this submitted manuscript and approved submission.

Research funding: The authors acknowledge the financial support from the DFG via grants HU2626/3-1(423427290), HU2626/6-1 (447515653), HU2626/5-1(445415315), SFB 1375 NOA (398816777) and HE5618/6-1.

Conflict of interest statement: The authors declare no conflicts of interest.

References

[1] Y. D. Chong, L. Ge, H. Cao, and A. D. Stone, "Coherent perfect absorbers: time-reversed lasers," *Phys. Rev. Lett.*, vol. 105, p. 053901, 2010.

[2] W. Wan, Y. Chong, L. Ge, H. Noh, A. D. Stone, and H. Cao, "Time-reversed lasing and interferometric control of absorption," *Science*, vol. 331, pp. 889–892, 2011.

[3] D. G. Baranov, A. Krasnok, T. Shegai, A. Alù, and Y. Chong, "Coherent perfect absorbers: linear control of light with light," *Nat. Rev. Mater.*, vol. 2, p. 17064, 2017.

[4] K. Pichler, M. Kühmayer, J. Böhm, et al., "Random anti-lasing through coherent perfect absorption in a disordered medium," *Nature*, vol. 567, pp. 351–355, 2019.

[5] W. R. Sweeney, C. W. Hsu, and A. D. Stone, "Theory of reflectionless scattering modes," *Phys. Rev.*, vol. 102, p. 063511, 2020.

[6] A. D. Stone, W. R. Sweeney, C. W. Hsu, K. Wisal, and Z. Wang, "Reflectionless excitation of arbitrary photonic structures: A general theory," *Nanophotonics*, vol. 10, pp. 343–360, 2021.

[7] J. Zhang, K. F. MacDonald, and N. I. Zheludev, "Controlling light-with-light without nonlinearity," *Light Sci. Appl.*, vol. 1, pp. e18–e18, 2012.

[8] S. Dutta-Gupta, R. Deshmukh, A. Venu Gopal, O. J. F. Martin, and S. Dutta Gupta, "Coherent perfect absorption mediated anomalous reflection and refraction," *Opt. Lett.*, vol. 37, pp. 4452–4454, 2012.

[9] H. Noh, Y. Chong, A. D. Stone, and H. Cao, "Perfect coupling of light to surface plasmons by coherent absorption," *Phys. Rev. Lett.*, vol. 108, p. 186805, 2012.

[10] J. W. Yoon, G. M. Koh, S. H. Song, and R. Magnusson, "Measurement and modeling of a complete optical absorption and scattering by coherent surface plasmon-polariton excitation using a silver thin-film grating," *Phys. Rev. Lett.*, vol. 109, p. 257402, 2012.

[11] R. Bruck and O. L. Muskens, "Plasmonic nanoantennas as integrated coherent perfect absorbers on SOI waveguides for modulators and all-optical switches," *Opt. Express*, vol. 21, pp. 27652–27661, 2013.

[12] M. J. Jung, C. Han, J. W. Yoon, and S. H. Song, "Temperature and gain tuning of plasmonic coherent perfect absorbers," *Opt. Express*, vol. 23, pp. 19837–19845, 2015.
[13] T. Roger, S. Vezzoli, E. Bolduc, et al., "Coherent perfect absorption in deeply subwavelength films in the single-photon regime," *Nat. Commun.*, vol. 6, p. 7031, 2015.
[14] X. Fang, K. F. MacDonald, and N. I. Zheludev, "Controlling light with light using coherent metadevices: all-optical transistor, summator and invertor," *Light Sci. Appl.*, vol. 4, pp. e292–e292, 2015.
[15] R. Alaee, Y. Vaddi, and R. W. Boyd, "Dynamic coherent perfect absorption in nonlinear metasurfaces," *Opt. Lett.*, vol. 45, pp. 6414–6417, 2020.
[16] N. Engheta, A. Salandrino, and A. Alù, "Circuit elements at optical frequencies: nanoinductors, nanocapacitors, and nanoresistors," *Phys. Rev. Lett.*, vol. 95, p. 095504, 2005.
[17] A. Alù and N. Engheta, "Input impedance, nanocircuit loading, and radiation tuning of optical nanoantennas," *Phys. Rev. Lett.*, vol. 101, p. 043901, 2008.
[18] J.-J. Greffet, M. Laroche, and F. Marquier, "Impedance of a nanoantenna and a single quantum emitter," *Phys. Rev. Lett.*, vol. 105, p. 117701, 2010.
[19] J.-S. Huang, J. Kern, P. Geisler, et al., "Mode imaging and selection in strongly coupled nanoantennas," *Nano Lett.*, vol. 10, pp. 2105–2110, 2010.
[20] L. Novotny, "Effective wavelength scaling for optical antennas," *Phys. Rev. Lett.*, vol. 98, p. 266802, 2007.
[21] S. Zhang, H. Wei, K. Bao, et al., "Chiral surface plasmon polaritons on metallic nanowires," *Phys. Rev. Lett.*, vol. 107, p. 096801, 2011.
[22] C. Rewitz, T. Keitzl, P. Tuchscherer, et al., "Ultrafast plasmon propagation in nanowires characterized by far-field spectral interferometry," *Nano Lett.*, vol. 12, pp. 45–49, 2012.
[23] Z. Zhu and T. G. Brown, "Full-vectorial finite-difference analysis of microstructured optical fibers," *Opt. Express*, vol. 10, pp. 853–864, 2002.
[24] R. L. Olmon, B. Slovick, T. W. Johnson, et al., "Optical dielectric function of gold," *Phys. Rev. B*, vol. 86, p. 235147, 2012.
[25] J.-S. Huang, T. Feichtner, P. Biagioni, and B. Hecht, "Impedance matching and emission properties of nanoantennas in an optical nanocircuit," *Nano Lett.*, vol. 9, pp. 1897–1902, 2009.
[26] G. Razinskas, P. Biagioni, and B. Hecht, "Limits of Kirchhoff's laws in plasmonics," *Sci. Rep.*, vol. 8, p. 1921, 2018.
[27] E. S. Barnard, J. S. White, A. Chandran, and M. L. Brongersma, "Spectral properties of plasmonic resonator antennas," *Opt. Express*, vol. 16, pp. 16529–16537, 2008.
[28] E. Feigenbaum and M. Orenstein, "Ultrasmall volume plasmons, yet with complete retardation effects," *Phys. Rev. Lett.*, vol. 101, p. 163902, 2008.
[29] J. Dorfmüller, R. Vogelgesang, R. T. Weitz, et al., "Fabry-pérot resonances in one-dimensional plasmonic nanostructures," *Nano Lett.*, vol. 9, pp. 2372–2377, 2009.
[30] T. H. Taminiau, F. D. Stefani, and N. F. van Hulst, "Optical nanorod antennas modeled as cavities for dipolar emitters: evolution of sub- and super-radiant modes," *Nano Lett.*, vol. 11, pp. 1020–1024, 2011.
[31] E. S. Wegert and Gunter, "Phase plots of complex functions: A journey in illustration," *Not. AMS*, vol. 58, pp. 768–780, 2011.
[32] A. Krasnok, D. Baranov, H. Li, M.-A. Miri, F. Monticone, and A. Alú, "Anomalies in light scattering," *Adv. Opt. Photonics*, vol. 11, pp. 892–951, 2019.
[33] R. F. Oulton, V. J. Sorger, T. Zentgraf, et al., "Plasmon lasers at deep subwavelength scale," *Nature*, vol. 461, pp. 629–632, 2009.
[34] Y.-J. Lu, J. Kim, H.-Y. Chen, et al., "Plasmonic nanolaser using epitaxially grown silver film," *Science*, vol. 337, p. 450, 2012.
[35] H. Park, S.-Y. Lee, J. Kim, B. Lee, and H. Kim, "Near-infrared coherent perfect absorption in plasmonic metal-insulator-metal waveguide," *Opt. Express*, vol. 23, pp. 24464–24474, 2015.
[36] I. Ament, J. Prasad, A. Henkel, S. Schmachtel, and C. Sonnichsen, "Single unlabeled protein detection on individual plasmonic nanoparticles," *Nano Lett.*, vol. 12, pp. 1092–1095, 2012.
[37] P. Zijlstra, P. M. Paulo, and M. Orrit, "Optical detection of single non-absorbing molecules using the surface plasmon resonance of a gold nanorod," *Nat. Nanotechnol.*, vol. 7, pp. 379–382, 2012.
[38] V. R. Dantham, S. Holler, C. Barbre, D. Keng, V. Kolchenko, and S. Arnold, "Label-free detection of single protein using a nanoplasmonic-photonic hybrid microcavity," *Nano Lett.*, vol. 13, pp. 3347–3351, 2013.

Supplementary Material: The online version of this article offers supplementary material (https://doi.org/10.1515/nanoph-2021-0048).